Quantum Electron Transport in Carbon Nanotubes: Velocity Oscillations and Length Dependence

Akin Akturk, Gary W. Pennington, Neil Goldsman
Department of Electrical and Computer Engineering
University of Maryland
College Park, MD 20742, USA
{akturka,garyp,neil}@glue.umd.edu

Alma E. Wickenden
Army Research Laboratory
2800 Powder Mill Road
Adelphi, MD 20783

***Abstract*— We report Monte Carlo simulation results that show position-dependent velocity oscillations and length effects in semiconducting single-walled zig-zag carbon nanotubes shown in Fig. 1. The simulations show velocity oscillations with Terahertz frequencies, which approach phonon frequencies; and velocity values reaching 7x10^7 cm/s. Simulations also show that average velocity overshoots and then decreases as the tube length increases. Quantum effects due to the finite length of the tubes, as well as radial confinement are also included in our Monte Carlo simulations.**

Keywords; Carbon nanotube, velocity oscillation, Terahetz frequency, monte carlo simulation

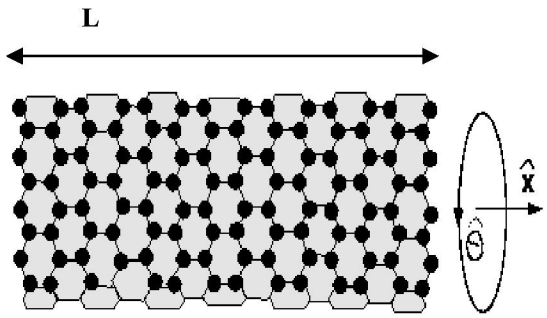

Figure 1. A single-walled zig-zag carbon nanotube, with fundamental indices n,m=0, and length L.

I. INTRODUCTION

Recently, carbon nanotubes (CNTs), which are graphite sheets (graphene) rolled up into tubes of nanometer scale diameters, have emerged as potential candidates for use in future nanoscale electronics [1], to overcome scaling problems associated with silicon-based devices. They offer a new design paradigm for electronics, mainly due to their electrical characteristics such as electron velocities approaching 1x10^8 cm/s at high fields, and 1x10^7 cm/s at low fields. This indicates very high low-field electron mobilities: More than ten-to-fifty times higher than that in silicon [1-3]. In addition, they are structurally strong with a high Young's modulus in TPa range, and form an inert surface with periodic boundary conditions, which improves transport properties. Furthermore, CNT electrical characteristics can be tuned for particular applications such as rectifying and current conduction. More specifically, the diameter and wrapping angle of a CNT determines its electrical characteristics including metal or semiconductor behavior. (A CNT can also be described by its fundamental indices (n,m), which are functions of the tube's diameter and wrapping angle.)

In this work, we investigate electron transport in semiconducting single-walled zig-zag CNTs, using a Monte Carlo (MC) simulator [1,2]. Our MC simulations indicate that we have spatial velocity oscillations, which imply Terahertz frequencies due to phonon scattering. Additionally, the wavelengths of these oscillations appear to depend linearly on the applied bias. Even though these calculated oscillations are observed in space, they are likely to cause oscillations in time due to dipole formations along the length of the tube, as is happening in Gunn diodes. To show if this is indeed the case, transient simulations need to be employed. Thus, our simulation results show that CNTs may open new paradigms in voltage-controlled oscillators, and RF designs in long-wave infrared.

Our calculated MC results also show that average CNT electron velocity as a function of tube length first increases with tube length (corresponding to the ballistic regime), overshoots, and finally reaches its steady-state phonon scattering-limited value for long tubes. In addition, our electric field versus applied field curves for infinitely long tubes exhibit negative differential velocities (NDV), similar in that respect to GaAs, where conduction velocity of the first subband is lower than that of the second due to differences in effective masses.

II. CARBON NANOTUBE MODEL

A. Monte Carlo for Long Tubes: The Continuum Model

To investigate the electron transport characteristics in a semiconducting single-walled zig-zag CNT with indices of n and m=0, we developed a Monte Carlo simulator [1,2]. Using our MC simulator, we obtain average ensemble electron velocities in CNTs, as a function of tube length and applied field.

To be used in our MC simulator, we first determine the CNT energy-momentum relations including electron and phonon energy dispersion curves. To obtain these curves, we use graphene's energy spectra, calculated using a tight binding model. Since CNTs are periodically confined graphite sheets

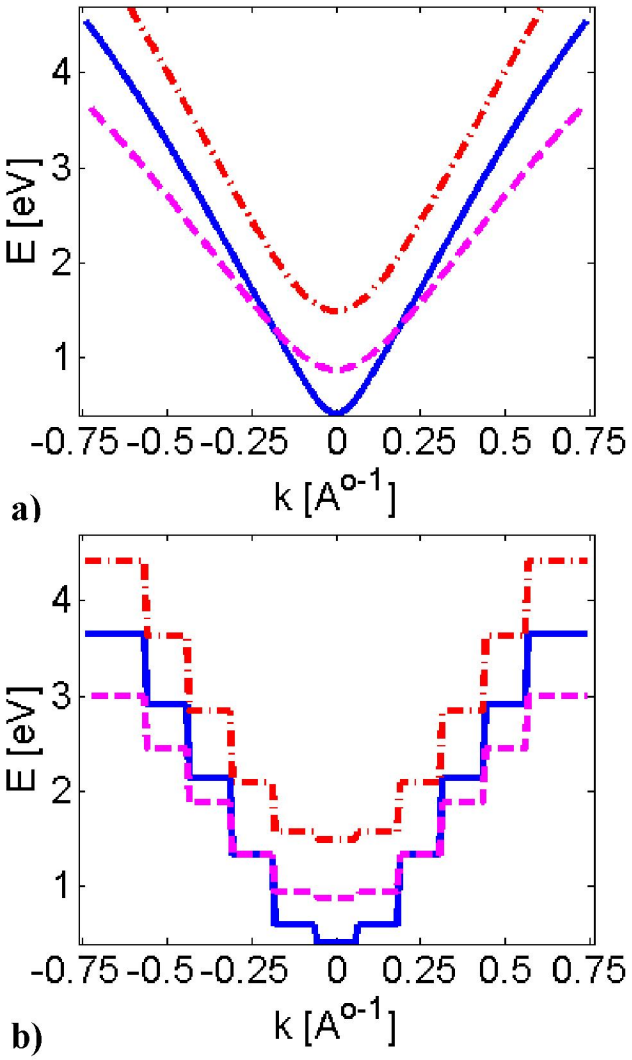

Figure 2. **a)** Energy dispersion relations for the first three subbands of an infinitely long n=13 CNT. **b)** Discretization of the energy dispersion curves of a 5nm long n=13 CNT (T= 4..31 A°).

due to rolling into a tube, CNT spectra were obtained by applying zone-folding methods to graphene energy dispersion relations. We below show the resulting energy-momentum relations for different CNT (n,0) subbands, distinguished by a subband index, β:

$$E = \gamma\sqrt{1 \pm 4\cos\left(\frac{\sqrt{3}}{2}ak_x\right)\cos\left(\frac{\pi\beta}{n}\right) + 4\cos^2\left(\frac{\pi\beta}{n}\right)} \quad \text{(eV)} \qquad (1)$$

Here, k_x (or k) is the electron momentum along the tube; a (= 2.49 Å) is the lattice constant of two dimensional graphite; and γ is the nearest-neighbor π-hopping integral taken to be 3 eV [4].

The CNT energy-momentum relation given in (1) is for tubes of infinite length. It is also a good approximation for tubes that are several times longer than the translational unit vector. In particular, CNT length divided by the length of the translational vector, which is equal to $\sqrt{3}a$ (= 4.31 A°), gives the number of unit cells on the tube. Therefore, it indicates how good the continuous band approximation is.

B. Finite CNT Length: Incorporating Quantization Effects

In addition to confinement around the circumference, we also consider effects due to finite lengths of the tubes, which lead to discretization in energy dispersion curves, as shown in Fig. 2b. For a zig-zag tube, length of the translational vector is roughly 4.31 A°, which is the distance between two parallel sides of the hexagon that forms the graphene. Therefore, maximum electron momentum is equal to π (pi) over this value, which is approximately 0.74 $A^{\circ-1}$. Furthermore, minimum momentum step is related to the length of the tube, which is 2π/L. Figure 2 shows the steps we have for a 5 nm length tube. We here have about eleven steps that correspond to the approximate ratio of 5 nm over 0.43 nm. Also, for the longest tube we simulate, which is 100 nm long, we have about twenty times more steps. (100 nm over 0.43 nm is roughly 232.) Using this information, we include the finite contribution of longitudinal quantization on electron transport during our simulations. We calculate scattering rates using the continuous band. We have modified our MC simulator to account for the quantization due to length in addition to circumference. In our modified MC, electron drifts along the length of the tube until it hits an energy barrier, like the steps shown in Fig. 2b, that needs to be overcome to achieve higher momentum values. At this point, we determine reflection and transmission probabilities for this barrier using the current energy, and barrier height. Depending on the likelihood of transmission, it either continues gaining momentum until it hits the next step or reflects back to negative momentum values. The longer the CNT, the smaller the barriers become, with the reflection coefficient approaching zero and the continuum approximation for long tubes.

C. Phonon Specra and Scattering Rates

To determine the CNT phonon spectra, we use a recipe similar to that used for obtaining the continuum model described before. More specifically, we start from the phonon dispersion curves of graphene. We then apply zone folding methods to those curves, and cut slices depending on the tube's diameter and wrapping angle. To facilitate faster computation of momentum and energy values that satisfy conservation laws, we approximate these slices using line segments.

After we obtain electron and phonon dispersion curves, we calculate electron-phonon scattering rates, employing the deformation potential approximation and Fermi's golden rule [2]. According to Fermi's golden rule; scattering rate from k to k' can be written as follows:

$$\Gamma_{kk'} = \frac{2\pi}{\hbar}|V|^2\,\delta\left(E_{k'} - E_k \pm E_p\right) \qquad (2)$$

Above delta function explicitly shows the energy conservation during absorption or emission. In addition, we write $|V|^2$ using deformation potential, as follows:

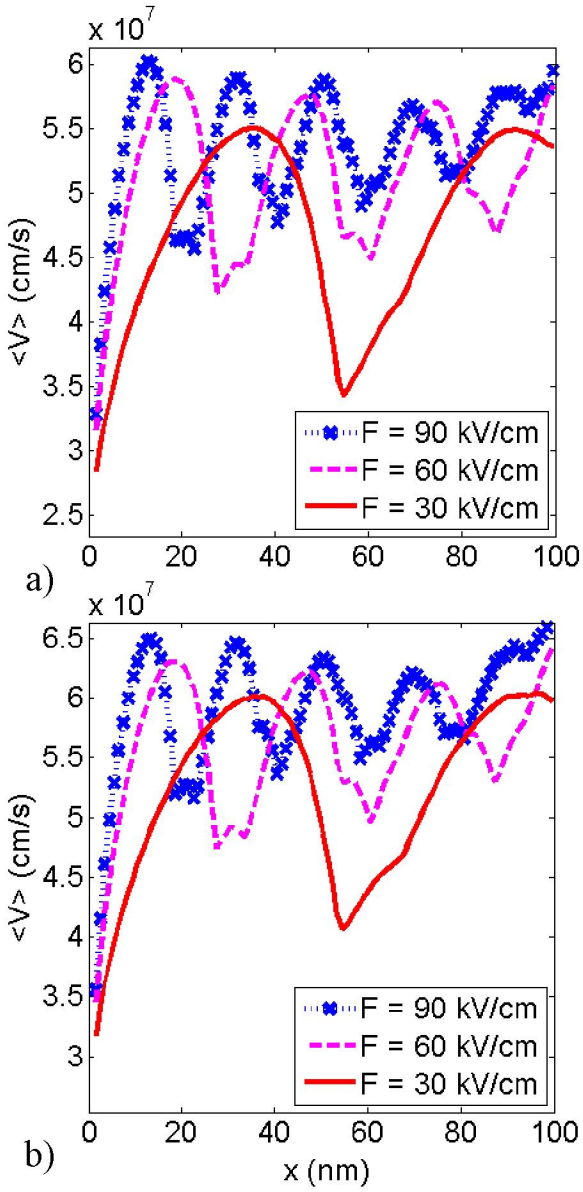

Figure 3. Average local electron velocities on 100 nm-long CNTs with indices of **a)** 13 and **b)** 16.

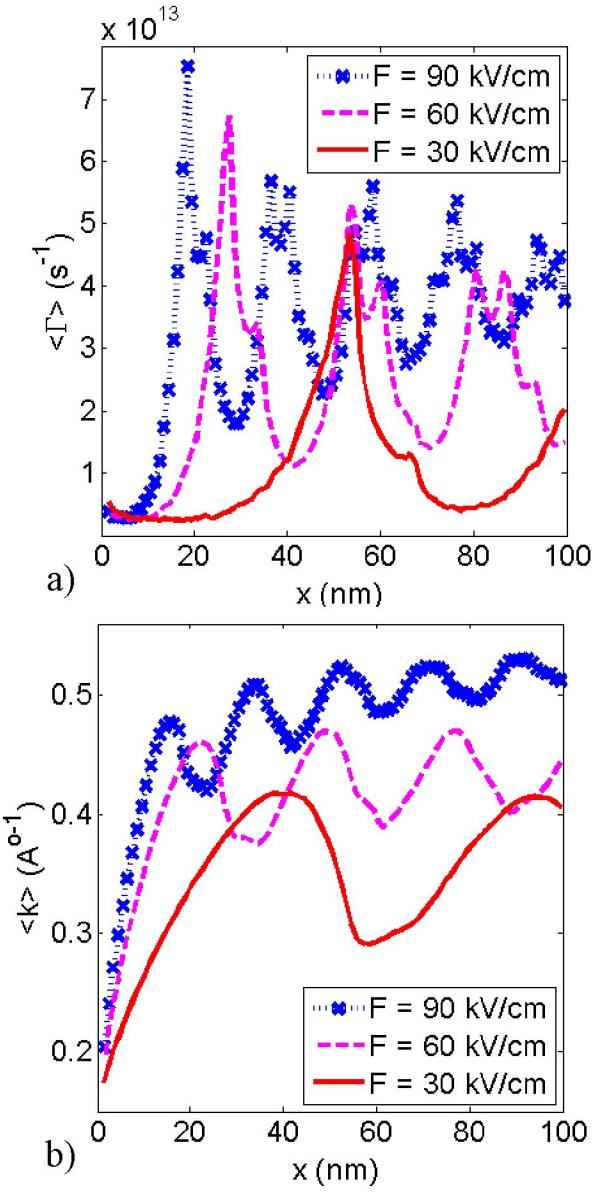

Figure 4. Average local **a)** scattering rate and **b)** momentum for n=13 tube under F = 30, 60, 90 kV/cm.

$$|V|^2 = \frac{\hbar^2 D^2 Q^2}{2L\rho E_p}\left[N_q \pm \frac{1}{2}\right] \tag{3}$$

Here, D is the deformation potential taken to be 3γ (= 9 eV); Q is a wavevector; ρ is the CNT linear mass density; E_p is a phonon energy; and the term in brackets is the Bose-Einstein phonon occupation number. Moreover, to calculate the total scattering rate from k to any other state, we integrate (2) over one-dimensional momentum space.

III. Simulation Results

Using our Monte Carlo simulator, we first investigate the location dependence of the CNT electron velocities as a function of applied field. To obtain electron velocity versus tube location statistics, we inject electrons with energies that are chosen from a probability density function of Fermi-Dirac distribution. Here, electrons are launched from both ends of the tube. Once they are in the tube, we record their position, average energy and momentum until they exit the tube from one end. Furthermore, to calculate average electron velocity in a space interval, we either keep track of the net momentum (Δk) and energy (ΔE) change in that interval, or the time spent (τ). Once we know these values, we calculate average velocity in that space interval using $\Delta E/\hbar\Delta k$ or ℓ/τ, which both gives the same value for average velocity.

We show in Figs. 3a and 3b our calculated average electron velocities on 100 nm-long CNTs. (In Fig. 3a, the CNT has a tube index and approximate diameter of 13 and 1 nm. On the other hand, in Fig. 3b, the CNT has a tube index and approximate diameter of 16 and 1.3 nm.) Our simulations show

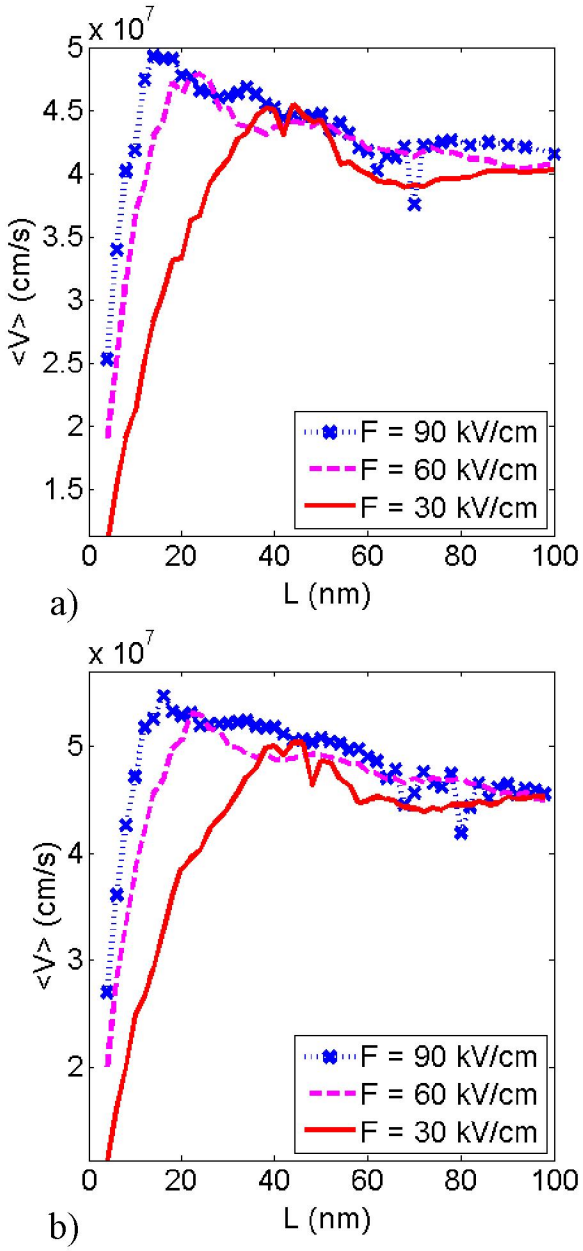

Figure 5. Average velocity of an electron on various length CNTs with indices of a) 13 and b) 16.

velocity oscillations corresponding to Terahertz frequencies in the frequency domain. In Fig. 3a and 3b, the highest oscillation frequencies are roughly 27 THz and 30 THz, respectively. We below show how we calculate the oscillation frequency for the tube (n= 13) in Fig. 3a for an applied field of 90 kV/cm:

$$f = \frac{v}{\lambda} = \frac{5.5\times10^{7}\,\text{cm/s}}{20\times10^{-7}\,\text{cm}} \simeq 27\ \text{THz} \qquad (4)$$

For the tube in Fig. 3b (n= 16), under the same field of 90 kV/cm, we have an oscillation frequency of 30 THz with the same average wavelength as in (4), but a higher average velocity of $6\times10^{7}\,\text{cm/s}$.

We associate this with the phonon spectrum and one-dimensional nature of the system, which results in the average scattering rates and momentums that are shown in Figs. 4a and 4b. More specifically, Fig. 4a shows that average scattering rate has two mixed oscillations with wavelengths of 18 nm and 22 nm, when the external field is 90 kV/cm. In addition, the peaks of these oscillations coincide with the local average electron velocity minimums in Fig. 3a. To understand why this happens, we first note that the energy of an electron drifting in an applied field of 90 kV/cm will increase by 160 meV and 200 meV after a free flight of 18 nm and 22 nm, respectively. These energy thresholds are critical in the sense that they correspond to energy differences sufficient enough to enable intervalley acoustic and optical, and intravalley and intervalley optical phonon emissions. Since the scattering rates associated with these phonons are high, electrons are highly likely to scatter once they have that much additional energy. Also, we know that the energy of an electron injected into the tube is likely to be around subband energy minimum due to Fermi-Dirac distribution. Therefore, after a flight of 18 nm or 22 nm, they will either scatter to subband energy minimum or higher energies. However, due to the one-dimensional nature of the CNT system, density of states of an electron peaks at subbands' minima with a $1/(E\text{-}E_{min})$ type of singularity. Thus, electrons are much more likely to scatter to lower momentum values where density of states peaks. This also causes oscillations in average local momentum curves shown in Fig. 4b for 100 nm long n=13 CNT under different applied fields. We also note that all or most of the electrons travel in the first subband, which eliminates the possibility to have the velocity oscillations due to transfer of electrons from the first to the second subband and vice versa.

In Fig. 5, we show our calculated average velocity for different CNT lengths. It shows how the forward and backward electron injections, initially, cancel each other out yielding an increase in electron velocity for an increase in length. We also have overshoots from a combination of the above mentioned scattering mechanism.

In summary, we calculate that the one-dimensional CNT system has velocity oscillations with Terahertz frequencies, which approach to those of phonons. This may facilitate very high frequency oscillators similar to Gunn diodes, opening new paradigms for far infrared RF electronics.

REFERENCES

[1] A. Akturk, N. Goldsman, and G. Metze, "Quantum modeling and proposed designs of carbon nanotube (cnt) embedded nanoscale mosfets," IEEE Trans. Elec. Dev., vol. 52, pp. 577-584, April 2005.

[2] G. Pennington, N. Goldsman, "Semiclassical transport and phonon scattering on electrons in semiconducting carbon nanotubes," Phys. Rev. B, vol. 68, pp. 45426-1-11, 2003.

[3] T. Durkop, S. A. Getty, E. Cobas and M. S. Fuhrer, "Extraordinary mobility in semiconducting carbon nanotubes," Nano Lett., vol. 4, pp. 35-39, 2004.

[4] R. Saito, M. S. Dresselhaus, and G. Dresselhaus, Physical Properties of Carbon Nanotubes, Imperial College Press, London, 1998.